Liquid Crystals
Publication details, including instructions for authors and subscription information:
http://www.informaworld.com/smpp/title~content=t713926090

Inversion walls in homeotropic nematic and cholesteric layers

J. M. Gilli; S. Thiberge; A. Vierheilig; F. Fried

Online publication date: 29 June 2010

To cite this Article Gilli, J. M. , Thiberge, S. , Vierheilig, A. and Fried, F.(1997) 'Inversion walls in homeotropic nematic and cholesteric layers', Liquid Crystals, 23: 5, 619 — 628

To link to this Article: DOI: 10.1080/026782997207894

URL: http://dx.doi.org/10.1080/026782997207894

LIQUID CRYSTALS, 1997, VOL. 23, NO. 5, 619–628

Inversion walls in homeotropic nematic and cholesteric layers

by J. M. GILLI*, S. THIBERGE, A. VIERHEILIG
Institut Non Linéaire de Nice, U.M.R. 129, CNRS, UNSA, 1361 Rte des Lucioles, 06560 Valbonne, France

and F. FRIED
Laboratoire de Physique de la Matière Condensée, CNRS, UNSA, Parc Valrose, 06108 Nice Cedex 2, France

(*Received 10 March 1997; accepted 13 May 1997*)

We describe the experimental properties of metastable domains associated with the presence of an Inversion Wall (IW) and observed with homeotropically anchored nematic and cholesteric liquid crystals sandwiched between parallel glass plates. Such a distorted situation, stabilized by the application of an electric field parallel to the plates as described in reference [1], can also be obtained transiently either when filling a sample cell by capillarity or in some studies of directional solidification at the N–I interface [2]. The application of an electric field perpendicular to the plates with $\Delta\varepsilon > 0$ materials allows control of the reversal region thickness in the bulk of the sample and its associated birefringence. This IW can be stabilized in the particular case of low lateral extension globules in which the line tension of the looped disclination separating the π wall regions from the homeotropic regions counter-balances the unfavourable bulk free energy. Particular attention is devoted to the defects of these walls, whose appearance using polarizing microscopy is similar to the umbilics of the Fréedericksz transition. The structure of these 'four brush' defects is nevertheless here singular, corresponding to point defects of a 3D uniaxial nematic medium. In the case of a chiral nematic, these IW undergo a particular undulation instability which is also observed in 2D simulations.

1. Introduction

From a fundamental point of view, it is known on one hand that nematic liquid crystal phases constitute a privileged medium for the investigation of line defect properties. On the other hand, walls and point defects have been much less investigated for this same medium (at least experimentally). We describe in the following a simple experimental situation allowing the observation and investigation of both these defect types.

As seen in figures 1 (*a*) and 1 (*b*), the spontaneous formation of IW metastable domains, that can be stabilized in the case of tilted anchorings [3], can be observed in the following simple experiments.

(1) By application of a strong electric field perpendicular to the plates, inducing the dynamic scattering mode (DSM), which leads, after relaxation, to an approximately equal surface ratio between normal homeotropic undistorted regions and such π IW.

(2) When glass plate cells, with treatment for homeotropic anchoring, are filled by capillarity: under shear flow, the director in a π IW profile is 'preferred' to a homeotropic profile. This effect results from the negative sign of the Leslie viscosity coefficient α_3; it occurs in most available nematic liquid crystals [4, 5].

(3) As previously described in the case of rapidly rotated magnetic fields [6], b-type domains of figure 1 (*b*), with double walls parallel to the plates, are obtained. Such domains also form when a system of two associated permanent magnets (leading to a sign change of the vertical field component) is moved in the observation area, as seen in figures 2 (*a*) and 2 (*b*), and a vertical electric field is abruptly applied to a $\Delta\varepsilon > 0$ material (figure 2 (*c*)). In this last case, the IW in fact constitutes a closed surface enclosing a topologically locked homeotropic volume which slowly shrinks.

Such surfaces are particular forms of 'membranes' with controllable thickness depending on the applied electric field (*thickness* $\approx 2\xi$ where ξ is the electric coherence length [7]). These 'membranes', immersed in a homeotropic bulk, necessarily possess an in-plane director and

*Author for correspondence.

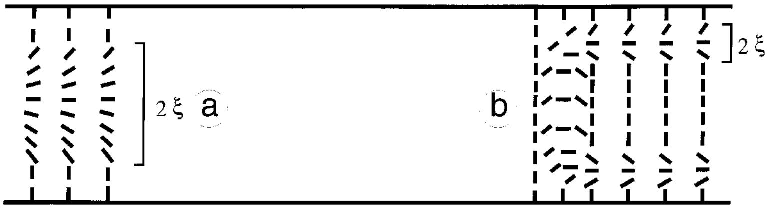

Figure 1. Reversal films parallel to the plates: (*a*) single and (*b*) double Neel films parallel to the glass plates in homeotropically anchored nematic samples.

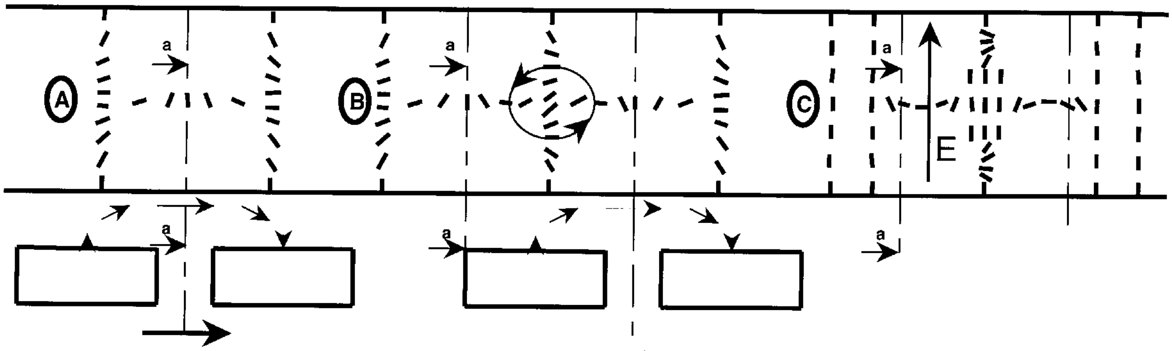

Figure 2. Formation of double Neel walls assisted by translating magnets. (A) The system of high field magnets produces curved flux lines; (B) displacement of the magnets induces a torque on the mid-plane directors and their tilt takes a value higher than π/2; (C) an abrupt application of an electric field increases this tilt up to π.

some of their properties can consequently be described in terms of a two-dimensional polar medium.

We describe in the following some observations on such membranes, such as for example the occurrence of point defects and 2D walls, and the behaviour of these defects under the influence of rotating magnetic fields as seen in photograph 3, 4 of figure 3. The particular case of such membranes, stabilized in small globules of nematic material under a rotating magnetic field, can be compared with recent observations on free-standing SmC smectic films by Cladis *et al.* [8, 9] or, more recently by us on SmC*.

2. Observations in extended samples

2.1. *Situations with single IW*

As observed in reference [10], when a sample of thickness d between parallel glass plates, suitably treated for homeotropic anchoring, is filled by capillarity, the homogeneous homeotropic texture is only obtained after the relaxation of the first formed transient metastable regions. Disclination lines of the type $\pm 1/2$ are present, parallel to the border region separating these metastable regions from the stable homeotropic domains. Our experiments, made with a positive dielectric anisotropy ($\Delta\varepsilon > 0$) material: 5CB (pentylcyanobiphenyl), reveal strong birefringence colour changes when a voltage between 0 and a few tens of V is applied perpendicularly to the plates.

We experimentally determine the thickness 2ξ of the turn-over region (figure (4)). At low field, this thickness tends to the separation d of the glass plates. For high fields, it tends to

$$2\xi = 2\frac{d}{V}\left(\frac{K}{\Delta\varepsilon}\right)^{1/2},$$

where K is a weighting average of K_{11} and K_{33}. An exact calculation of K is not the aim of this paper. The change of behaviour follows for $2\xi = d$

$$\left(\text{i.e. } \frac{1}{V} = \frac{1}{2}\left(\frac{\Delta\varepsilon}{K}\right)^{1/2}\right).$$

We found $2\xi = d$ for $1/V = 2{\cdot}0\ \mathrm{V}^{-1}$ which is in rather good agreement with the values found in the literature for elastic constants K_{11} and K_{33} and the dielectric anisotropy $\Delta\varepsilon$ [11]. The corresponding critical value of $1/V$ calculated with $K = K_{33}$ is shown in figure 4.

Considering a linearly polarized incident light wave and assuming that the angle ϕ between the director and the z axis varies linearly from 0 to π in the turn-over region 2ξ and vanishes elsewhere, the calculated optical phase difference between the ordinary and extraordinary rays is:

$$\Delta\Phi = \frac{2\pi}{\lambda}\int_0^{2\xi}\left(n_{e\parallel}\left(\pi\frac{z}{2\xi}\right) - n_o\right)\mathrm{d}z,$$

where

$$n_{e\parallel}(\phi)=\frac{n_o n_e}{(n_e^2\cos^2\phi+n_o^2\sin^2\phi)^{1/2}}$$

where n_e and n_o are the ordinary and extraordinary refractive indices.

The intensity of the transmitted light across the sample and the second polarizer vanishes when

$$2\xi=\frac{\lambda}{2}(2j+1)\frac{1}{\int_0^1 (n_{e\parallel}(\pi t)-n_o)\,\mathrm{d}t},$$

where j is an integer.

For a given wavelength, we measured voltages giving rise to extinction. Knowing the refractive indices, we deduced the value of 2ξ. This behaviour is comparable to that obtained in the case of the homeotropic Fréedericksz transition (HFT) in the high field region [7]: in this case, the birefringence variation simply originates from the thickness variation of the connecting regions, close to the glass plates. One difference here is the position of the reversal layer in the middle of the sample (the validity of this model is here enhanced at high fields, the anchoring strength on the glass plates not being involved).

Another way to obtain this IW consists in applying a strong electric field perpendicular to the plates on homeotropically anchored nematics, inducing a DSM2 turbulent texture. The relaxation of the electric field leads in this case to a sample surface in the IW state approximately equal to that in the homeotropic ground state, but with a random distribution. This case leads to a large number of defects, locked in the IW domains. These defects slowly annihilate in pairs as in the case of a classical electric field induced HFT, but these two situations are in fact rather different from a fundamental point of view. In the HFT case, close to the transition threshold, the experiment can be described by an X–Y model simply assuming the occurrence of the first unstable mode of deformation. The order parameter can thus be a vector (or a complex number) in a layer located in the mid-plane sample. Then, the static or dynamical behaviour of such a situation could be theoretically described within the framework of the Ginzburg–Landau (G–L) normal form approach, as presented in reference [12]. In this case, the observed defects (phase defects of the G–L equation) are the classical vortices of the X–Y model [13]. From the point of view of the 3D nematic, they are the two possible 'escaped' disclinations, the escape direction being perpendicular to the glass plates. In the present case, the mid-plane nature of the defects is relative to a 2D in-plane polar medium without the possibility of the third dimension 'escape'. From the point of view of the 3D nematic order, the observed defects now possess a singular nature: they are point defects characterized by a positive or negative integer rank. We will come back to the topology of these point defects in the section devoted to globules.

2.2. *Formation of IW assisted by a magnetic field*

As seen in figure 2, the application of an electric field perpendicular to the plates with a high enough magnetic field parallel to them, allows the formation of two π walls with opposed topology. The magnetic field strength condition arises from the fact that the director in the mid-plane of the sample must be close to the plate plane direction (figure 2 (*a*)). Then, a translation of the two permanent magnets, parallel to the plates, coupled with the curvature of the flux lines, gives rise to a torque exerted on the molecules (figure 2 (*b*)). In the surface region swept by the magnet displacement, this torque causes the molecules to tilt more than the $\pi/2$ value corresponding to saturation of the Fréedericksz transition. If we now abruptly apply a strong electric field perpendicular to the plates, the mid-plane region of the sample tilts further to reach a value close to π and it is now separated from the top and bottom glass plates by two π walls of opposite sense (figure 2 (*c*)) having, as previously described, a 2ξ thickness and being separated by a homeotropic orientation (figure 5).

In all our experiments, these two charge walls of opposite topology never annihilate as indicated in reference [6] by a simple recombination during the time allowed for the observation: this time is clearly limited by the progressive shrinking of these domains that are always unfavourable relative to the lower energy homeotropic ground state. Consequently, an interesting question arises from this fact: are the two π walls close to the plates interacting through some undetermined repulsive force of an electric or other nature, or is the recombination time associated with low attractive forces (exponential decay) very long compared with the border shrinking time? This remains an open question to which we will try to respond by increasing the size of our sample and by eliminating dust particles that also clearly favour the nucleation of homeotropic normal domains.

3. IW in small sized globules

3.1. *Experimental and topological studies*

Figures 6 (*a*) and 6 (*b*) correspond to a third simple situation in which the π reversal domains are stabilized in cylindrical globules of small extension. Such globules are easily obtained from an initially normal homeotropic nematic sample with a thickness ranging from ten to a few hundred micrometers, just by injecting compressed air in between the glass plates: the liquid crystal is expelled for the most part and only small globules with

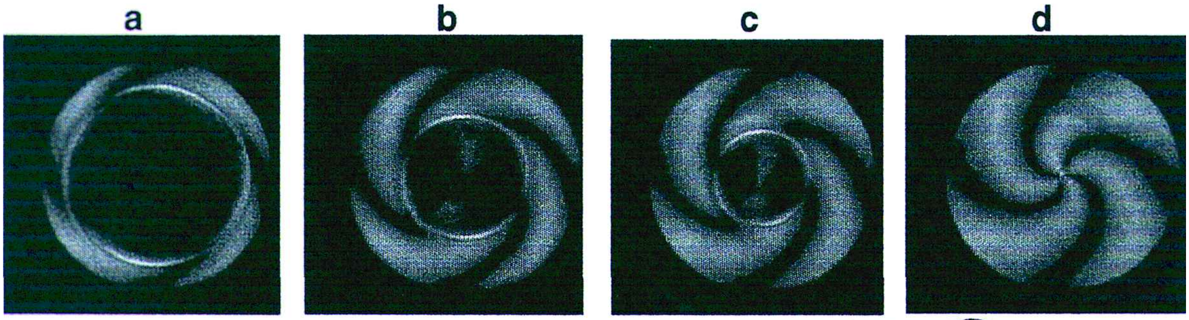

Photograph 1 polars orientation:

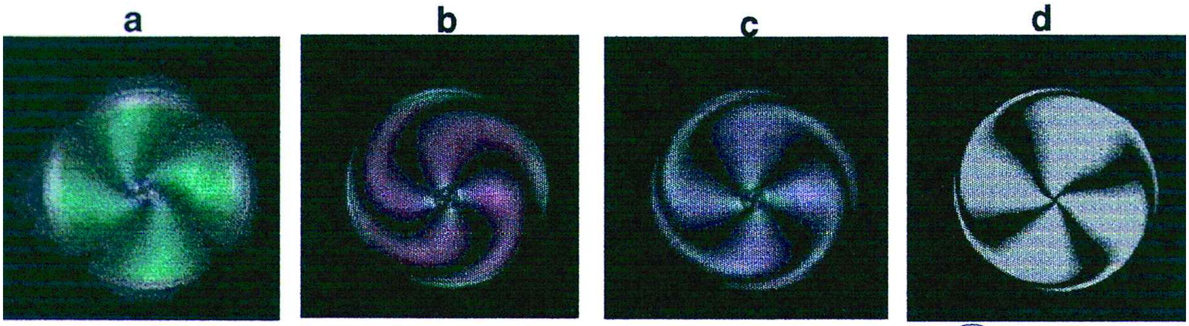

Photograph 2 polars orientation:

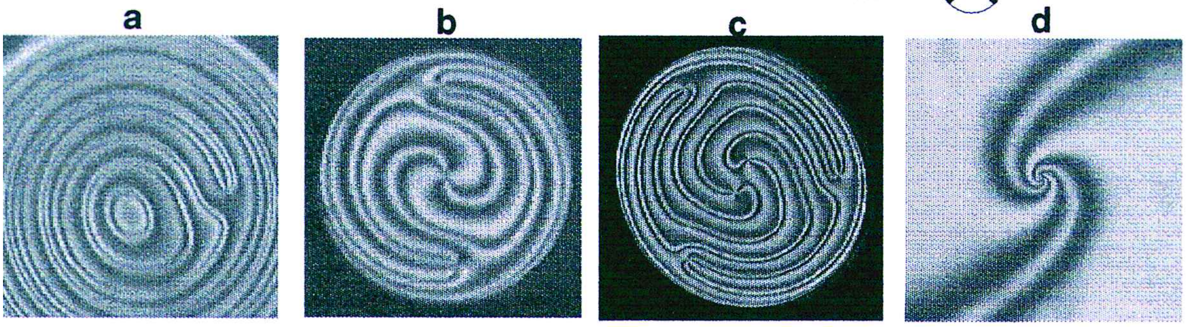

Photograph 3

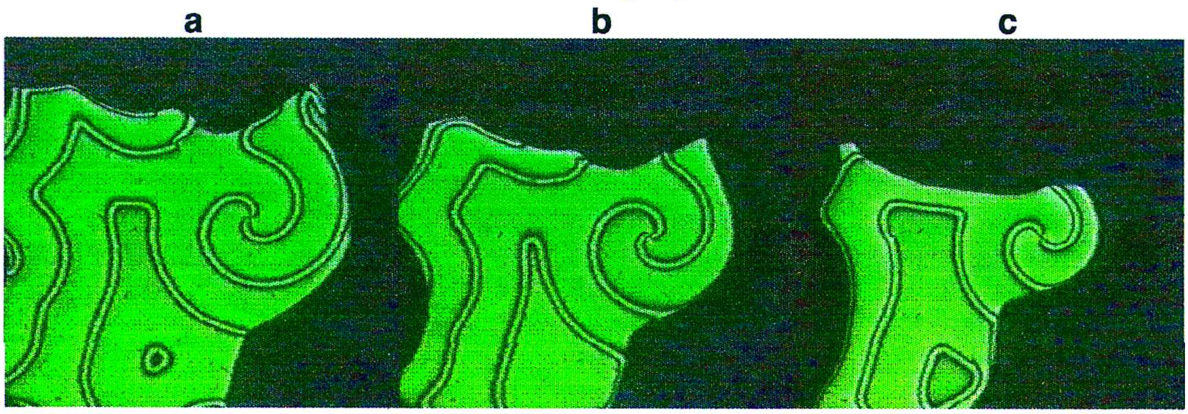

Photograph 4

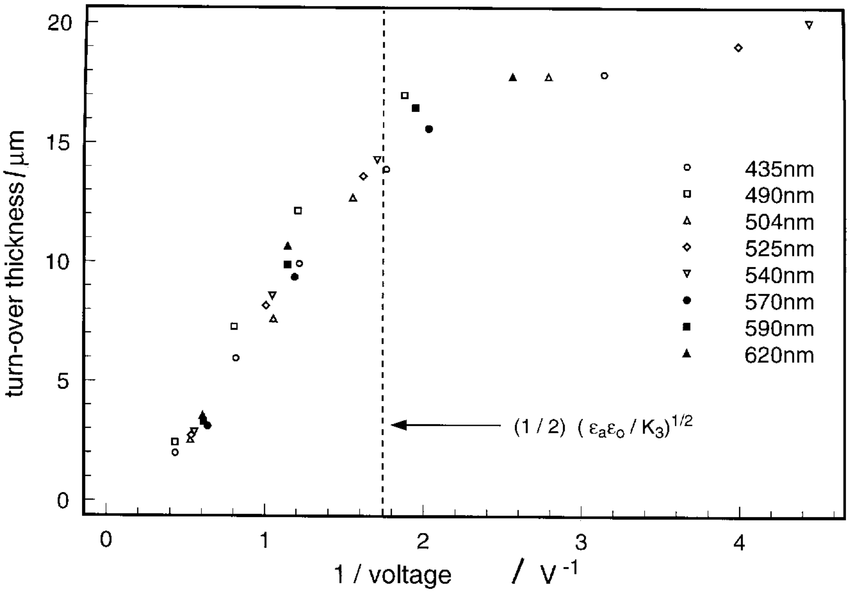

Figure 4. Experimental thickness of turn-over region as deduced from birefringence measurements at different wavelengths versus the inverse applied voltage. The sample thickness was 23 microns.

different diameters remain visible in the microscope field of view. After some relaxation, one can observe that only the smaller droplets remain bright or coloured between crossed polarizers over their complete extent as in photographs 1d and 2 of figure 3.

The larger globules are black in their central region, indicating a homeotropic organization. For these large globules, the outer region close to the meniscus keeps the same aspect as for the smallest globules. In this case, the two (homeotropic and bright) regions are separated by a more or less circular ring corresponding to a looped disclination (figure 6 (*a*) and photographs 1a, b, c of figure 3).

The observation of these two globule types with different structures clearly defines a critical radius r_0 for the globules (or more precisely for the looped disclination line): (i) if the radius is larger than r_0, the loop increases its size and stays close to the meniscus whose topology favours the reversal region; (ii) if the radius is lower than r_0, the loop shrinks slowly to a point defect of $+1$ charge as seen in figure 6 (*b*), and photograph 1 of figure 3. We attribute a $+1$ charge to this point defect, although this is just a matter of convention. This comes from the fact that the hedgehog point defect often observed in capillary experiments (glass tubes with homeotropic condition [14]) is, to our knowledge, generally associated (by convention) with a $+1$ topological charge. If we now come back to our original experimental situation (nematic between homeotropically anchored glass plates with a metastable π reversal of the director when going from the upper to the lower plate), we can build a defect having exactly the same physical structure (hedgehog) close to the director singularity (in our small extension globule situation, this hedgehog defect would be built naturally with a reversed curvature meniscus). We consequently attribute by convention the same $+1$ charge to this defect. The structure in figure 6 (*b*), corresponding to the air–liquid meniscus,

Figure 3. Photograph 1: as for all the following photographs, photograph 1 was taken with the sample between crossed polarizers. Time evolution of a small diameter globule ($\Phi \approx 100\,\mu$m) showing the progressive shrinking of the looped disclination, lowering the energy cost of the singular line and forming the point defect in c. The spiral shape of the brushes is, as in figure 6, associated with the twist, present in the neighbourhood of the looped line or point defect. Photograph 2: small diameter globule transformation under the influence of an increasing voltage applied perpendicular to the plate with positive dielectric anisotropy material. Photograph 3: large diameter globules (a:$\Phi \approx 500\,\mu$m, b:$\Phi \approx 200\,\mu$m) and the effect of a rotating magnetic field; (a) the ± 1 point defect initially present in the centre of the globule rotates on a particular orbit, screening the continuous phase winding of the central region relative to the elastically locked outer region; (b, c) in the presence of an odd number of defects greater than one, the n '-1' defects rotate in the centre of the globule and the $n+1$ '$+1$' defects rotate on an outer orbit with reverse senses; (d) ($50\,\mu$m $\times$ $50\,\mu$m) relaxation of the winding—due to the elastic anisotropy of the nematic free energy, the '$+1$' defect remains preferentially in its twist configuration and the phase unwinding results in the accumulation of deformation close to the defect. Photograph 4: time evolution of a single IW domain slowly shrinking in the presence of an in-plane rotating magnetic field; the initial presence of point defects and walls results in the formation of spiral waves.

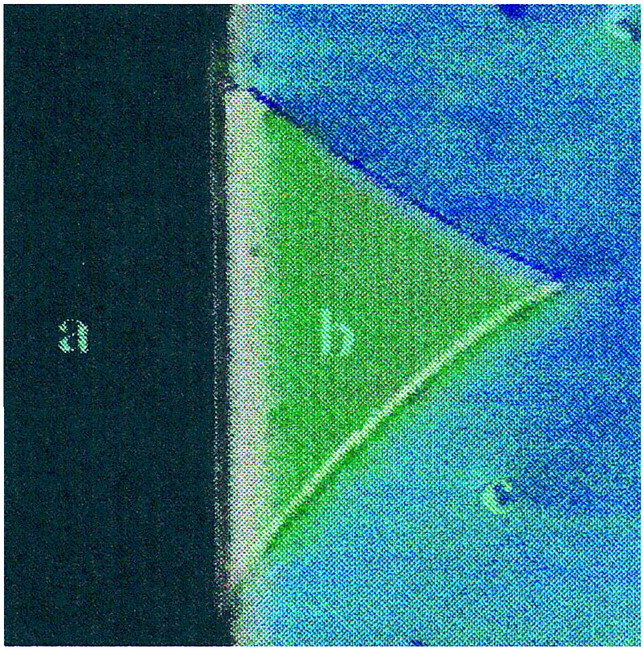

Figure 5. Photograph of a 'scratched' double Neel film slowly shrinking: regions a, b and c correspond, respectively, to the ground state homeotropic geometry, a double π wall and a π wall.

can be obtained from the hedgehog defect via a continuous transformation (a simple rotation of all the molecules relative to the z direction, orthogonal to the plates), a transformation that is still allowed while maintaining the 'base point' defined on the boundary. So the defect can be associated with a +1 charge. The −1 defects have the same physical structure, but with orientation of the asymptotic line parallel to the plate, and cannot continuously transform into this last situation without changing the orientation of the 'base point'.

3.2. *Effect of an electric field perpendicular to the plates*

In our experiments performed on a $\Delta\varepsilon > 0$ material (pentylcyanobiphenyl), we investigated the effect of variable electric fields on the disclination loop and the point defect structure. The quantitative results and the fits with potential models involving volume free energy and line tension are described in detail in reference [15]. The main results are the following.

An increasing electric field applied perpendicularly to the plates makes the reversal domain situation less and less favourable (the volume free energy difference between the π reversal region and the lower energy homeotropic region scales with the electric field E). The looped disclination line is consequently repelled closer to the meniscus and the measured outward speed of this line also increases.

Starting from a small globule ($r < r_0$) with a point defect, we can observe a simple situation allowing for a controlled topological transformation between point and looped line defect [16]. The reverse transformation can also be observed at low or zero electric field, starting from small globules. These two opposed transformations reveal some high energy barrier rendering difficult the

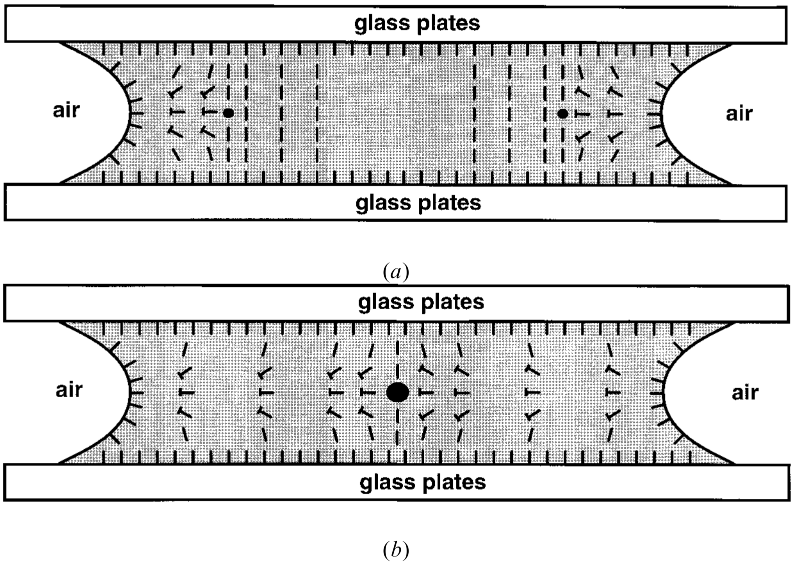

Figure 6. Nails schemes of a globule in a diametrical cut perpendicular to the glass plates. (*a*) A looped disinclination line separates the homeotropic central region of the globule from the IW outer region; (*b*) a point defect is seen in the centre. In both the cases, some twist is introduced in the upper and lower regions of the globule, this being associated with expenditure of some bend in the mid-plane of the sample, as seen from the spiral shape of the extinction brushes of photographs 1 and 2 of figure 3.

point–loop transformation that needs an electric field of the order of 25 000 V cm^{-1} or more. The application of such high voltages also reveals striking features in the transitional structure of the globule as seen in photographs 2 of figure 3.

Starting from small globules initially having four extinction brushes between crossed polarizers, the voltage is progressively increased: at low voltages, the brushes present a more or less spiral shape of random sense, indicating a rotation of the mid-plane director on going from the point defect to the meniscus region. This rotation lies between $-\pi/2$ and $\pi/2$ and probably comes from the elastic anisotropy; some free energy can be gained in the upper and lower neighbourhood of the singular point by introducing some twist deformation. An interesting and misunderstood behaviour arises when the field is strongly increased from this situation. The birefringence of the reversal domain falls to a low value giving rise to a grey Newton tint, but the brushes which are still visible strongly modify their shape and the function describing the rotation of the mid-plane director is now complex (photograph 2d of figure 3). The initial phase variation of this director ($\pi/2 > \theta > -\pi/2$) is now concentrated close to the meniscus and a reverse variation of the phase is observable in the main part of the globule. This behaviour is possibly related to the increase in range of decay of the perturbation associated with the defect presence [17].

3.3. *Effect of a rotating magnetic field in the plane of the glass plates*

The application of a high enough frequency magnetic field rotating in-plane allows the collapse of the loop disclination even in large globules ($r > r_0$). As remarked in reference [18], in the limit of infinite frequency of rotation, an in-plane magnetic field is equivalent to the effect of an electric field perpendicular to the plates on a $\Delta\varepsilon < 0$ material, which favours an in-plane orientation of the director. The π wall domain is consequently favoured in this case and we use this process experimentally to obtain rather large globules with a point defect topology. In general, a frequency of rotation of a few Hz is sufficient to achieve this effect. At lower frequency, as well as in the presence of an in-plane static magnetic field, the looped line becomes strongly distorted with two cusps in the magnetic field direction. This is easily explained from the necessary change of twist sign at the cusp which is a high energy edge defect region. When the field rotates, the elongated loop rotates itself or the cusp often remains stuck on the meniscus rendering the collapse impossible.

If we now focus our observations on the point defect globules, whatever process is used to obtain them, the rotating field gives rise to transient winding of the director. When an electric potential of a few volts is applied simultaneously to a $\Delta\varepsilon > 0$ material, the observed phenomena are particularly simple and described by a two-dimensional analysis. We can associate the formation of targets or highly wound spiral shaped brushes as the simple phase winding of the director in the mid-plane of the sample. If we start from the situation of the $+1$ defect in the centre of the globules, and wind the 'phase' with the help of a relatively 'low intensity', 'high frequency' magnetic field, the $+1$ point defect remains in the centre of the globule, but the phase is wound in steps around it; an energy barrier associated with the twist, splay–bend organization change must be overcome to obtain the winding. Strictly speaking, in the mid xy-plane of the sample, we get a pure bend deformation, but above and below it, where the tilt angle of the director from the z axis is between 0 and $\frac{\pi}{2}$ we have a sufficiently strong twist deformation to get qualitatively the same effects as in the $+1$ line defect case. With a high enough magnetic field and a low enough rotation speed, the $+1$ point defect is expelled from the centre and begins to orbit around it (photograph 3a of figure 3). In this way, it relaxes the phase by moving on a circle with a radius depending on the experimental parameters. In the equilibrium state, during one revolution of the vortex, four dark rings are created in the centre corresponding to a phase creation of 2π. In the presence of several vortices in large globules, we get a stationary state with one or several vortices of the same sign in a small orbit (usually -1 vortices) and the corresponding number of vortices of opposite sign in large orbit (photographs 3b, c of figure 3). Note that the sum of the topological charges of all vortices is still $+1$. In the case of a small globule and a single vortex in the inner orbit, its radius may be very small.

When turning off the rotating magnetic field, the system relaxes and in the presence of several vortices, they will annihilate. In the case of one single $+1$ vortex, it moves to the centre and rotates to relax the phase. Once more, the rotation of the $+1$ vortex takes place in distinct steps between the two different stable configurations and just before such a step the distortion near the vortex becomes very strong (photograph 3d of figure 3).

When an in-plane, rotating magnetic field is now applied on slowly shrinking IW of large extension, possessing some point defects as obtained through the application of a high voltage electric field (DSM2), spiral waves having an appearance similar to the HFT case [12, 19], are formed (photograph 4 of figure 3).

4. IW in the case of a cholesteric liquid crystal

In the case of chiral nematics, it is also possible to obtain the IW by experiments comparable to those previously described. As in the nematic cases, we used $\Delta\varepsilon > 0$ materials. For a rather high voltage, the IW a b c

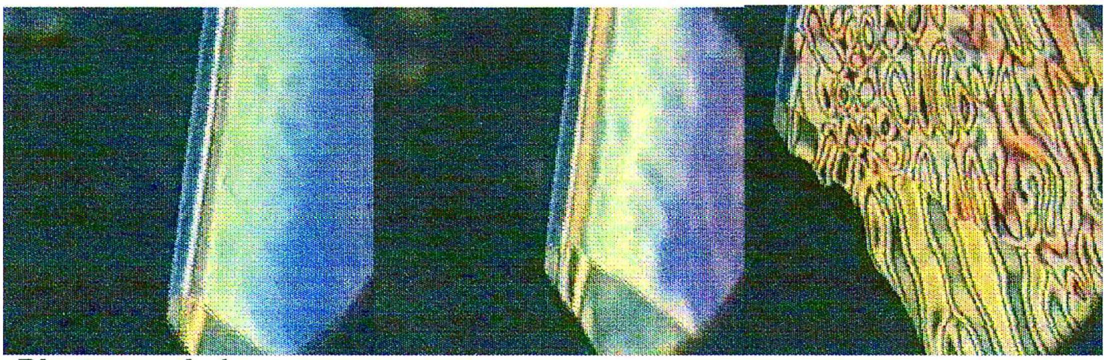

Photograph 1

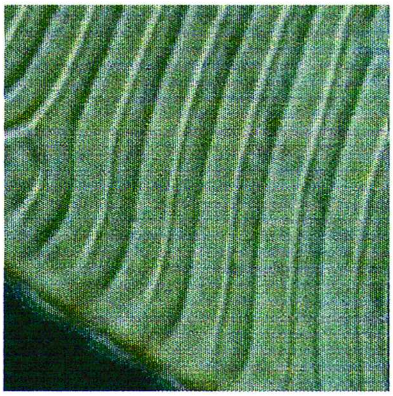

Photograph 2

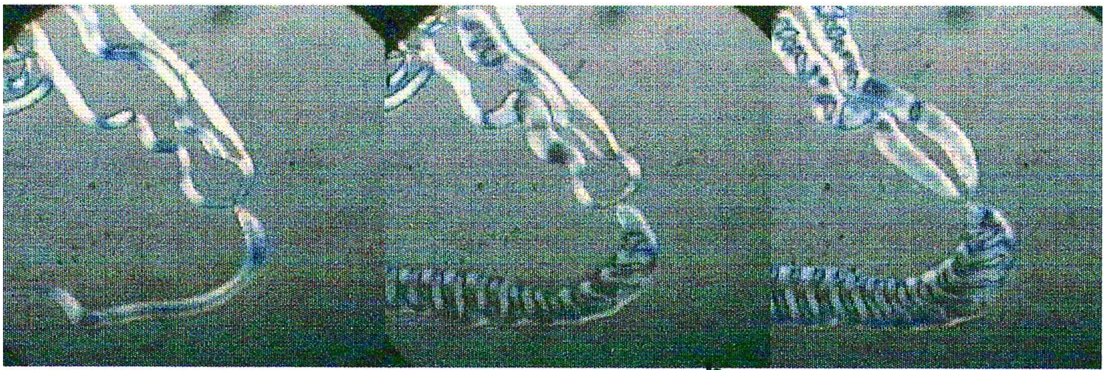

a Photograph 3 b c

Photograph 4

polars orientation:

Photograph 5

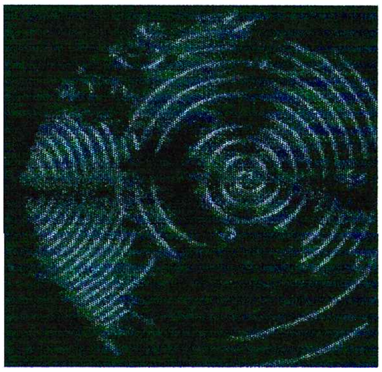

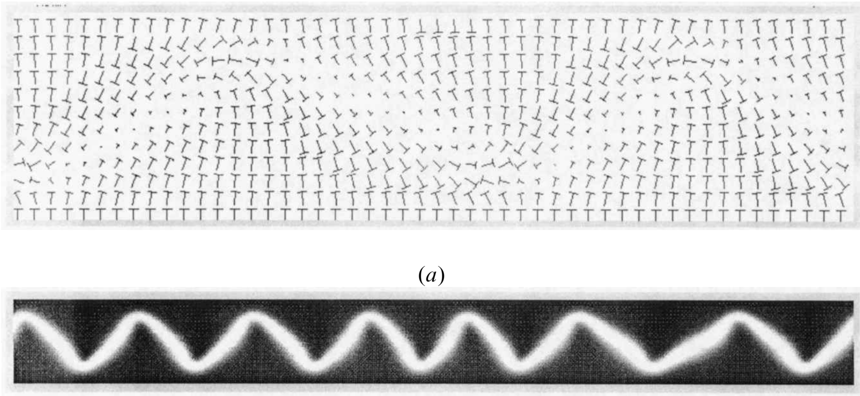

(*a*)

(*b*)

Figure 8. Courtesy of L. Gil: Ginzburg–Landau simulation of IW perpendicular to the plate in a chiral situation. (*a*) Nail convention scheme showing the periodic instability corresponding to the introduction of some twist parallel to the plates; (*b*) amplitude of the director component perpendicular to the cut; the symmetry breaking along the cut and the non-sinusoidal shape of the undulation are clearly visible here.

domains obtained are homogeneous, as in the pure nematic case (photograph 1 of figure 7). The only difference is the nature of the colours observed which clearly demonstrate the presence of rotatory power across the film due to the conical twist, perpendicular to the plates. Moreover, this conical twist can be seen from the grey aspect of the brushes: due to the rotatory power, the black extinction brushes observed with pure nematics between crossed polarizers become grey in chiral systems. This difference decreases at very high voltage, the optical rotation decreasing with the thickness of the reversal region. If the voltage perpendicular to the plate is decreased starting from this homogeneous situation, a striped instability appears abruptly as observed on photograph 1c of figure 7. Simulations of the Ginzburg–Landau equation made on 2D cuts ([20] figure 6) of the samples are in qualitative agreement with this phenomenon; moreover they reveal a striking feature of the instability. This modulation of the reversal region, clearly associated with the introduction of a twist deformation parallel to the plates, is not of a sinusoidal nature, but introduces a symmetry breaking as in the case of the teeth system of some carnivores. This modulated reversal domain seems, in some particular experimental situation associated with the presence of a well defined frequency a.c. electric field [20], to lose its metastable nature and become favoured compared with the homeotropic situation (photograph 2 of figure 7). In particular, the domains of a reversal film, with or without dynamic modulations, can develop from the ribbon structures described in reference [20] as seen in photograph 3 of figure 7. Photographs 4 and 5 show that the ribbon structure, probably associated with a propagating oblique IW, can develop in the shape of rotating archimedian spirals [21]. As suggested by the referee, an interesting open question concerns the wavelength selection of the structure observed numerically in figure 8 and experimentally in photographs 1c, 2, and 3b and c of figure 7. Up to now, our studies have been made with a confinement ratio $C = d/P$ close to 1 and in this case the period of the instability is, as expected, of the same order as the thickness d and the pitch P. Work is actually now in progress to investigate how this wavelength is selected at high values of C.

5. Conclusion

We have described some experimental properties of metastable IW domains in homeotropically anchored

Figure 7. Photograph 1: (1 mm × 1 mm), $d \approx 50\,\mu$m, sample between crossed polarizers. Double IW in the presence of chirality when the voltage applied perpendicular to the plate is abruptly decreased from homeogeneous situation (figure 2(*c*)); appearance of an undulation of the walls. Photograph 2: (120 μm × 120 μm), $d \approx 20\,\mu$m. The same pattern as that obtained from a ribbon in the presence of an a.c. electric field perpendicular to the plate (see photograph 3 of figure 7); in that case the domain does not shrink spontaneously. The optical modulation perpendicular to the stripes is compatible with the simulation results of figure 8. Photograph 3: (1 mm × 1 mm), polarizers uncrossed. The spontaneous transformation of a ribbon into a striped structure; as for photograph 2, the stripes move perpendicular to their axes. Photograph 4: (1 mm × 1 mm). Formation of a four arm archimedian spiral in a cholesteric material under the influence of an a.c. electric field; the arm of the spiral is constituted by the ribbon. Photograph 5: (3 mm × 3 mm). The spiral waves of reference [21] close to the cholesteric–SmA transition are probably also constituted by the same low extension oblique IW ribbon structure.

nematic liquid crystals. We have described the different mechanisms to obtain this configuration of the director and measured the thickness of the turn-over region as a function of the electric field applied to a 5CB sample.

The globules allow the study of point defects. At low voltage, a rotation of the director in the mid-plane of the sample, along a radius of a globule is observed. When a high field is applied, the initial rotation of the director is now concentrated close to the meniscus and a reversed variation of the phase is observed in the main part of the globule. This surprising behaviour is not yet understood.

The study of globules also constitutes a simple experiment allowing for a controlled topological transformation between a looped line defect and a point defect. We have shown the existence of a critical radius for the looped line defect, allowing the measurement of the line energy [15]. The application of a rotating magnetic field to globules with a turn-over of the director and a +1 defect gives rise to phase winding of the director. Targets associated with an orbiting defect similar to those observed in SmC samples by Cladis *et al.* [8], and the formation of several orbiting defects are observed. These configurations are stationary states, chosen by the system to relax phase winding due to the rotating magnetic field.

In the case of a cholesteric liquid crystal material, some new features such as an original symmetry breaking modulation are observed in agreement with Ginzburg–Landau simulations. Because turn-over of the director is located in the mid-plane of the sample and the thickness is easily controlled, the extended IW surfaces could be of technological interest. As preliminarly observed by us, IW formed with polymer liquid crystals with a glass transition above room temperature lead to the fabrication of well controlled birefringent solid films.

We thank L. Gil for allowing us to mention the numerical simulations results and J. Fehrenbach for helpful discussions. We also acknowledge the DRET administration (94-2610A) and The University of Nice for financial support.

References

[1] Cladis, P. E., Saarloos, W., Finn, P. L., and Kortan, A. R., 1987, *Phys. Rev. Lett.*, **58,** 222.
[2] Bechhoefer, J., 1988, PhD thesis, University of Chicago, USA.
[3] Komitov, L., Hauck, G., and Koswig, H. D., 1986, *Phys. Stat. Solids (a)*, **97,** 645.
[4] Gahwiller, C., 1972, *Phys. Rev. Lett.*, **28,** 1554.
[5] Gleeson, J. T., Palffy-Muhoray, P., and van Saarloos, W., 1991, *Phys. Rev. A*, **44,** 2588.
[6] Heppke, G., and Schneider, F., 1974, *Z. Naturforsch*, **29a,** 310 and 1356.
[7] De Gennes, P. G., 1974, *The Physics of Liquid Crystals* (Oxford: Clarendon Press).
[8] Cladis, P. E., Finn, P. L., and Brand, H. R., 1995, *Phys. Rev. Lett.*, **75,** 1518.
[9] Cladis, P. E., Couder, Y., and Brand, H. R., 1985, *Phys. Rev. Lett.*, **55,** 2945.
[10] Pieranski, P., private communication.
[11] Bunning, J. D., Faber, T. E., and Sherrell, P. L., 1981, *J. Physique*, **42,** 1175.
[12] Gilli, J. M., Morabito, M., and Frisch, T., 1994, *J. Phys. II Fr.*, **4,** 319; Frisch, T., Coullet, P., Rica, S., and Gilli, J. M., 1994, *Phys. Rev. Lett.*, **72,** 1471.
[13] Rapini, A., 1973, *J. Physique*, **34,** 629.
[14] Williams, C. E., Pieranski, P., and Cladis, P., 1972, *Phys. Rev. Lett.*, **29,** 90.
[15] Buka, A., Chevallard, C., Gilli, J. M., and Thiberge, S., (to be published).
[16] Mori, H., and Nakanishi, H., 1988, *J. Phys. Soc. Jpn.*, **57,** 1281.
[17] Kramer, L., private communication.
[18] Leger-Quercy, L., 1976, PhD thesis, University de Paris-Sud.
[19] Migler, K. B., and Meyer, R. B., 1991, *Phys. Rev. Lett.*, **66,** 1485; Migler, K. B., 1991, PhD thesis, Brandeis University, Boston, USA; Migler, K. B., and Meyer, R. B., 1994, *Physica D*, **71,** 412.
[20] Gil, L., 1995, *J. Phys. II Fr.*, **5,** 1819.
[21] Gilli, J. M., and Kamaye, M., 1992, *Liq. Cryst.*, **11,** 791.